

# Calculation and experimental determination of damping properties for polymer composite material

Eremin V.P., Bolshikh A.A.  
Moscow Aviation Institute (National Research University),  
Moscow, Volokolamskoe shosse, 4, 125993  
Russia

Received: April 18, 2021. Revised: April 21, 2022. Accepted: May 16, 2022. Published: June 25, 2022.

**Abstract—** In all real materials, energy is dissipated during deformation. You can think of it as a kind of internal friction. The load curve for the full period does not fit into a straight line.

Usually, to describe the damping in the material, a model is used in terms of the hysteresis loss coefficient, since the energy losses per period depend weakly on frequency and amplitude. At the same time, the mathematical description in the loss factor model is based on complex values, that is, it implies only the case of harmonic vibration. Therefore, this damping model can only be used for frequency-domain studies.

Rayleigh damping is a simple approach to forming the damping matrix as a linear combination of the mass matrix and the stiffness matrix. This damping model is unrelated to any physical loss mechanisms.

In this paper, we consider a model of a mathematical pendulum for the experimental and computational determination of the damping properties of a polymer composite material. For the experimental part, a stand was designed and created that simulates the excitation of a plate made of a polymer material. The computational repetition of the experiment was performed by the finite element method and using the analytical Runge-Kutta method of the 4th and 5th order.

**Keywords—**Rayleigh damping model, natural frequency, damping ratio, finite element method, composite materials.

## I. INTRODUCTION

The free-oscillation method is based on the determination of the attenuation of free oscillations. Losses of cyclic

deformation arising under the influence of stresses are determined by the logarithmic decrement of damping of free vibrations [1-3]. The sample is given an initial oscillation amplitude and the number of times the damped oscillation amplitude decreases are recorded. At a small degree of deformation, the relative energy loss does not depend on the amplitude, which changes during damping.

The most common variation of the method is the use of a torsion pendulum. In this case, the sample in the form of a plate is the elastic part of the pendulum. The period of oscillation of a torsion pendulum can be changed by varying the moment of inertia of the weights suspended on the plate. The method of internal friction is based on the use of free torsional vibrations, for which GOST 20812-83 defines a frequency range of 0.1 ... 27 Hz. For this purpose, direct-type torsion pendulums are used.

Before testing, the linear dimensions of the samples are measured. The thickness is measured at least five places along the entire length of the specimen and is calculated as the arithmetic mean. The largest and smallest values may deviate from the average value by no more than 3%, otherwise, the sample cannot be accepted for testing.

The sample is fixed in the upper and lower clamps of the device so that its longitudinal axis coincides with the axis of the oscillatory system to obtain strictly sinusoidal oscillations.

After fixing the sample, its length is measured between the clamps with an error of not more than 0.1 mm.

By removing the load from the rest position, the system is brought into oscillatory motion. The angle of twist during oscillation should not exceed 3° in each direction. The frequency and amplitude of oscillations are recorded using a measuring system, the measurement results are recorded in an

electronic journal.

## II. EXPERIMENTAL DETERMINATION OF THE DAMPING PROPERTIES OF THE MATERIAL

**Description of the experiment.** The experimental stand is shown in Fig. 1.

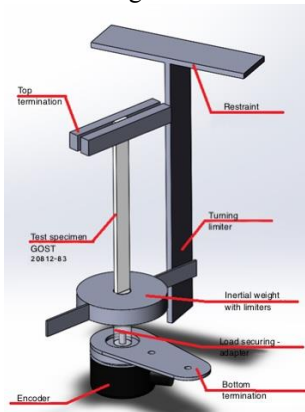


Fig. 1 diagram of the torsion pendulum

The inertial part is a round metal disk with a certain moment of inertia, the mass and dimensions of which are chosen so that the tensile stress on the sample does not exceed 0.1 MPa.

Clamps must provide reliable coaxial fastening of the sample, have a small mass and a negligible moment of inertia, which can be neglected. Fixing the sample should not affect the measurement results [4-8].

The collection of information about the change in the angle of twist of the pendulum is carried out using the encoder and the digital system ZETSensor connected to it Fig. 2, which collects data from the primary analog converters and transmits a digital signal to the PC.



Fig. 2 measuring equipment ZETSensor

**Description of the test bench.** The test bench is a structure that has a vise with slots for fastening to the welding table and a U-shaped console for mounting measuring equipment. The sample is fixed in a vice in the lower part of the stand, on the upper part, it is attached to the encoder through a sleeve, to which, in turn, a weight is attached [9]. The test stand is shown

in Fig. 3

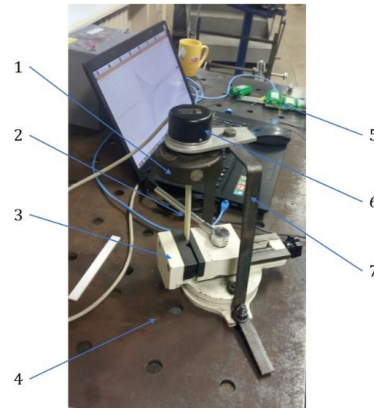


Fig. 3 test bench

Table 1 presents the names of the elements indicated in Fig. 3.

Table 1. Test bench elements	
Item element	Element name
1	Weight
2	Test sample
3	Vice clamps
4	Welding table
5	Measuring equipment
6	Encoder
7	U-shaped console

**Analysis of test results.** The result of the tests is a plot of the sample twist angle versus time at a frequency of 200 Hz Fig. 4.

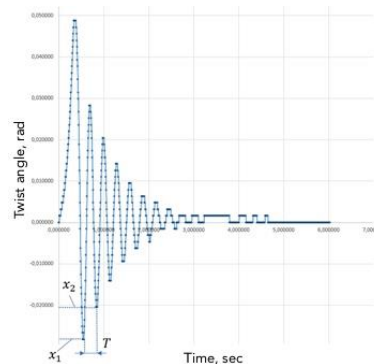


Fig. 4 test result

The tests were carried out 4 times for one sample. The test results are presented in Table 2.

Table 2. Test result

Test num ber	Angle value at the first point ( $X_1$ ), degree	Angle value at the second point ( $X_2$ ), degree	Time value at the first ( $t_1$ ) point, sec	Time value at the second ( $t_2$ ) point, sec
1	1.53	1.17	21.209	21.525
2	2.07	1.53	19.950	20.260
3	1.62	1.17	17.558	17.870
4	1.89	1.35	20.980	21.280

After testing, the obtained data are analyzed, the period and frequency of attenuation oscillations and the logarithmic decrement of attenuation are calculated. Consider the calculation of these parameters for the first test.

The damping oscillation period is:

$$T = t_2 - t_1 = 21.525 - 21.209 = 0.316 \text{ sec}$$

The damping oscillation frequency is:

$$\omega = \frac{2 \cdot \pi}{T} = \frac{2 \cdot 3.14}{0.316} = 19.883 \text{ Hz}$$

The logarithmic decrement is equal to:

$$\delta = \ln \left( \frac{X_1}{X_2} \right) = \ln \left( \frac{1.53}{1.17} \right) = 0.268$$

The results of the analysis of the remaining tests were calculated similarly and are presented in Table 3 [10].

Table 3. Test result

Test number	Value of oscillation damping period ( $T$ ), degree	Value of oscillation damping frequency ( $\omega$ ), degree	Value of the logarithmic damping decrement ( $\delta$ ) point, sec
1	0.316	19.883	0.268
2	0.310	20.268	0.302
3	0.312	20.138	0.325
4	0.300	20.944	0.336
Average value	0.310	20.309	0.308

### III. DETERMINATION OF THE DAMPING PROPERTIES OF THE MATERIAL BY THE FINITE ELEMENT METHOD ACCORDING TO THE RAYLEIGH DAMPING MODEL

**Definition of coefficients of proportionality.** To simulate the damping properties of the material, the Rayleigh damping model is used - the proportional damping model:

$$C = \alpha \cdot M + \beta \cdot K,$$

where  $C$ ,  $M$ ,  $K$  are global matrices of damping, mass, and stiffness,  $\alpha$  is a constant characterizing inertial damping,  $\beta$  is a constant characterizing structural damping.

The oscillation damping coefficient can be found in terms of natural circular frequency:

$$\zeta_i = \frac{\alpha}{2 \cdot \omega_i} + \frac{\beta \cdot \omega_i}{2}, \quad (1)$$

where  $\omega_i$  – natural circular frequency of the sample

The main advantage of this method is that it models the damping parameters for the material and not for a specific structure, i.e. Having determined the damping parameters for a given sample, this model can be used to calculate other structures made from this material [11–13].

To determine the coefficients of proportionality  $\alpha$  and  $\beta$ , it is necessary to carry out a modal calculation to determine the natural frequencies of the sample corresponding to two different successive modes of vibration.

According to the results of the calculation for the test sample, such vibrations are torsional and bending vibrations, as shown in Fig. 5.

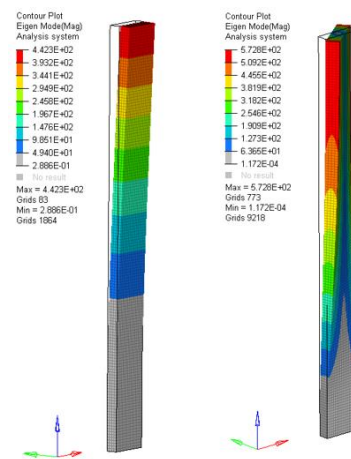


Fig. 5 analysis of the modes of vibration of natural frequencies

After determining the necessary modes of vibration, a calculation is carried out similar to the tests for the frequency shape corresponding to torsional vibrations, and the calculation for bending vibrations. For these two calculations, the same parameters of proportionality coefficients and material parameters are introduced to find the relationship between the logarithmic decrement of the damping of bending and torsional vibrations. The result of these calculations are graphs of the twist angle or sample displacement versus time,

similar to the graph shown in Fig. 4. Further, using the obtained dependence between the logarithmic damping decrement of torsional and bending vibrations and circular frequencies, the logarithmic decrement, and circular frequency are found, corresponding to bending vibrations for experimental calculations, because the existing stand can conduct tests corresponding only to torsional vibrations [14-16].

The oscillation damping coefficient can be expressed in terms of the logarithmic decrement:

$$\zeta = \frac{\delta}{2 \cdot \pi}, \quad (2)$$

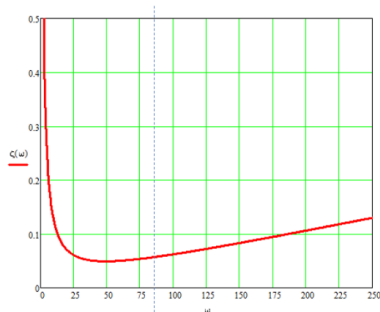


Fig. 6 the dependence of the attenuation coefficient of oscillations on the circular frequency

Using equations 1 and 2, it is possible to solve a system of equations corresponding to torsional (with index 2) and bending (with index 1) vibrations, for which all quantities will be known, except for the required proportionality coefficients  $\alpha$  and  $\beta$ :

$$\alpha = \frac{2 \cdot \omega_1 \cdot \omega_2 (\zeta_1 \cdot \omega_2 - \zeta_2 \cdot \omega_1)}{\omega_2^2 - \omega_1^2}$$

$$\beta = \frac{2 (\zeta_2 \cdot \omega_2 - \zeta_1 \cdot \omega_1)}{\omega_2^2 - \omega_1^2}$$

As a result of solving this system of equations, the following results were obtained:

$$\alpha = 2.413 \frac{1}{\text{sec}}$$

$$\beta = 0.001 \text{sec}$$

The function of the dependence of the attenuation coefficient on the circular frequency [1] has the form (Fig. 1.6). As you can see, this dependence can be divided into two parts (dashed line in Fig. 6), where the first part of the graph depends on the proportionality coefficient  $\alpha$ , and the second part, respectively, on the coefficient  $\beta$ , therefore, the coefficient  $\alpha$  is more responsible for the attenuation coefficient fluctuations in the range of small values of circular frequencies, and the coefficient  $\beta$ , respectively, in the range of

large values of circular frequencies [17].

**Description of the finite element model.** The parameters of the material of the sample are set the same as for the test sample. They are presented in table 4.

A finite element model (FEM) of a sample with given boundary conditions is shown in Fig. 1.7. The type of FE used to simulate the sample in this model is a shell element, the average size of the FE is 1 mm, the number of FEs is 2220. The weight is modeled by a rigid FE - rbe2 with given mass-inertia parameters presented in Table 5.

Table 4. Material parameters

Material	Modulus of elasticity, MPa	Poisson's ratio	Tensile strength, MPa	Density, tons/mm <sup>3</sup>
Fluoroplast - 4	725	0.4	11	$2.2 \cdot 10^{-9}$

Table 5. Mass-inertial indicators of the weight

Parameter	Value	Physical dimension
Weight	0.001	tons
Moment of inertia about the axis of rotation of a cylindrical weight	1.137	tons\mm <sup>2</sup>



Fig. 7 FEM for the analysis of damping properties

At one end of the sample, restrictions are imposed on all degrees of freedom (embedding) along with the length corresponding to fixing the sample in a vise during testing. A forced angular displacement is applied to an independent node of the element that simulates a weight, corresponding to the angle of twist of the sample during testing, at a time of 3 seconds, the forced displacement is removed.

**Analysis of the FEM calculation results.** The result of the calculation is the dependence of the sample twist angle on time (Fig. 8). After plotting the dependence, the damping parameters are determined. Decay oscillation period:

$$T = t_1 - t_2 = 0.516 - 0.797 = 0.281 \text{sec}$$

Decay oscillation frequency:

$$\omega = \frac{2 \cdot \pi}{T} = \frac{2 \cdot 3.14}{0.281} = 22.36 \text{ Hz}$$

Logarithmic decrement:

$$\delta = \ln \left( \frac{X_1}{X_2} \right) = \ln \left( \frac{0.041}{0.028} \right) = 0.358$$

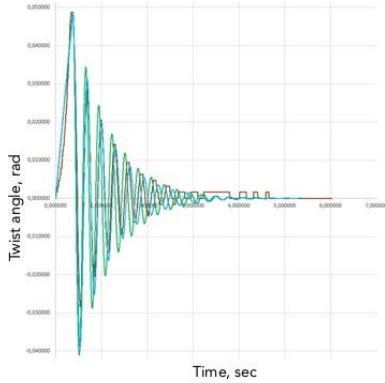


Fig. 8 the result of the FE calculation

#### IV. DETERMINATION OF THE DAMPING PROPERTIES OF THE MATERIAL BY THE ANALYTICAL METHOD

**Drawing up a differential equation.** A common matrix equation of dynamic equilibrium is compiled for the entire system:

$$M \cdot \ddot{\varphi} + C \cdot \dot{\varphi} + K \cdot \varphi = 0, \quad (3)$$

where  $C$ ,  $M$ ,  $K$  are global matrices of damping, mass,

and stiffness, respectively,  $\varphi$  is the sample twist angle.

Using the Rayleigh damping method, the damping matrix can be represented as:

$$C = \alpha \cdot M + \beta \cdot K, \quad (4)$$

where  $\alpha$  is a constant characterizing inertial damping,

$\beta$  is a constant characterizing structural damping [18].

Substituting Equation 3 into Equation 4, we get:

$$[M] \ddot{\varphi} + [\alpha[M] + \beta[K]] \dot{\varphi} + [K] \varphi = 0,$$

or

$$J_m \cdot \ddot{\varphi} + [\alpha \cdot J_m + K \cdot \beta] \dot{\varphi} + K \cdot \varphi = 0,$$

where  $J_m$  – total moment of inertia of the plate and weight.

As a result, the differential equation necessary for solving can be represented as:

$$\ddot{\varphi} + \left[ \alpha + \frac{K \cdot \beta}{J_m} \right] \dot{\varphi} + \left[ \frac{K}{J_m} \right] \varphi = 0, \quad (5)$$

**Determination of the missing data for solving the equation.** Next, you need to find the missing data, such as the total moment of inertia of the sample with a weight and the torsional stiffness of the system.

The initial data for the calculation are presented in Table 6.

Table 6. Initial data for calculation

Parameter	Value	Physical dimension
Plate thickness, $a$	4	mm
Plate width, $b$	15	mm
Plate length, $L_{plate}$	150	mm
Plate weight, $m_{plate}$	$1.98 \cdot 10^{(-5)}$	tons
Modulus of elasticity of the plate material, $E$	725	MPa
Poisson's ratio, $\nu$	0.4	-
Load weight, $m_{load}$	$1 \cdot 10^{(-3)}$	tons
Load radius, $r$	46	mm

First of all, the moments of inertia of the weight and the plate are found:

$$J_{load} = \frac{m_{load} \cdot r^2}{2} = 1.058 \text{ mm}^2 \cdot \text{tons}$$

$$J_{plate} = \frac{m_{plate} \cdot b^2}{12} = 3.713 \cdot 10^{-4} \text{ mm}^2 \cdot \text{tons}$$

The total moment of inertia is:

$$J_m = J_{load} + J_{plate} = 1.058 \text{ mm}^2 \cdot \text{tons}$$

To determine the polar moment of inertia, it is necessary to use a coefficient applicable for rectangular sections and depending on the ratio of the thickness and width of the sample [19]. For a given section, this coefficient is equal to:

$$B = 0.263$$

Next is the polar moment of inertia of the plate:

$$J_{polar} = B \cdot b \cdot a^3 = 252.48 \text{ mm}^4$$

The shear modulus for the plate material is determined by the formula:

$$G = \frac{E}{2(1 + \nu)} = 258.929 \text{ MPa}$$

By determining the shear modulus, you can find the torsional stiffness of the structure:

$$K = \frac{G \cdot J_{polar}}{L_{plate}} = 435.829 \frac{\text{H} \cdot \text{mm}}{\text{rad}}$$

**Solution of a differential equation.** The differential equation 5 was solved by the one-step explicit Runge-Kutta

method of the 4th and 5th order [20], the problem statement has the form shown in Fig. 9.

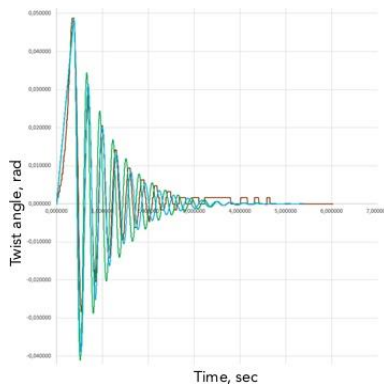


Fig. 9 solution of the equation

The input data for the calculation are the coefficients of proportionality, the values of which were determined in paragraph 1.2.1, the torsional stiffness of the plate, and the total moment of inertia of the weight together with the plate. In Fig. 1.9, A1 and A2 are the factors in front of  $\varphi'$  and  $\varphi$ , respectively:

$$A1 = \alpha + \frac{K \cdot \beta}{J_m}$$

$$A2 = \frac{K}{J_m}$$

**Analysis of the result of the analytical method of calculation.** The result of the analytical calculation is the dependence of the sample twist angle on time Fig. 10.

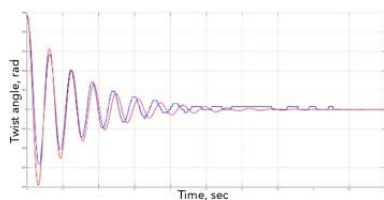


Fig. 10 results of the analytical method of calculation

Fig. 10 shows the resulting graph for the analytical calculation method (red graph) and the test results (blue graph).

After plotting the dependence, the damping parameters are determined.

Decay oscillation period:

$$T = t_2 - t_1 = 0.456 - 0.155 = 0.301 \text{ sec}$$

Decay oscillation frequency:

$$\omega = \frac{2 \cdot \pi}{T} = \frac{2 \cdot 3.14}{0.301} = 20.874 \text{ Hz}$$

Logarithmic decrement:

$$\delta = \ln \left( \frac{X_1}{X_2} \right) = \ln \left( \frac{0.391}{0.252} \right) = 0.439$$

## V. COMPARISON OF THE RESULTS OF ANALYTICAL CALCULATION AND FEM CALCULATION WITH EXPERIMENTAL DATA

**Comparative analysis of the results of analytical calculation and calculation of the FEM.** Comparative analysis of calculation results with experimental data is presented in Table 7.

Table 7. Comparison calculation results with experimental data

Calculation type	Value of oscillation damping period (T), degree	Value of oscillation damping frequency (ω), degree	Value of the logarithmic decrement (δ) point, sec
Experiment	0.310	20.309	0.308
FEM	0.281	22.360	0.358
Analytical	0.301	20.874	0.439

Fig. 11 shows the resulting graph for the analytical calculation method (blue graph), the test result (brown graph), and the finite element calculation result (green graph).

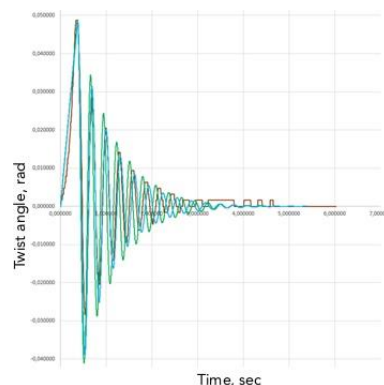


Fig. 11 comparison of calculation results

## VI. CONCLUSIONS AND RECOMMENDATIONS

As can be seen from the calculation results, the time from the beginning to the end of damping for all cases has approximately the same value. The values of the frequencies of the first oscillations are the same for all three cases, the differences from the experimental data begin to appear at small values of the plate twist angle.

The combined method for calculating coefficients of models  $\alpha$  and  $\beta$  for calculating Rayleigh damping can be applied at the stage of designing aircraft structures and thus obtain calculated results of static and dynamic accuracy of model determination.

In the future, the developed method is supposed to be used for constructively manufactured samples.



## References

- [1] E. Erduran, "Evaluation of Rayleigh damping and its influence on engineering demand parameter estimates," *Earthq. Eng. Struct. Dyn.*, vol. 41, 2012, pp. 1905–1919.
- [2] J. F. Hall, "Problems encountered from the use (or misuse) of Rayleigh damping," *Earthq. Eng. Struct. Dyn.*, vol. 35, 2006, pp. 525–545.
- [3] J. F. Hall, "Problems Encountered from the Use (or Misuse) of Rayleigh Damping," *Earthq. Eng. Struct. Dyn.*, vol. 35(5), 2005, pp. 525–545.
- [4] W. Heylen, S. Lamens and P. Sas, "Modal analyses. Theory and testing," Leuven. University. Leuven., 2003, 325 p.
- [5] D.J. Ewins, "Modal testing: Theory, practice and application," – 2nd ed. (Baldock: Research Studies Press LTD), 2000.
- [6] F. Zareian and R. A. Medina, "A practical method for proper modeling of structural damping in inelastic plane structural systems," *Comput. Struct.*, vol. 88, 2010, pp. 45–53.
- [7] P. Olsen, M. Juul and R. Brincker, "Condensation of the correlation functions in modal testing," *Mech Syst Signal Process*, vol. 118, 2019, pp. 377–387.
- [8] N. Jamil, A.R. Yusoff and M.H. Mansor, "Response prediction of static modal testing on milling machine tool," *Appl. Mech. Mater.*, vol. 606, 2014, pp. 131–135.
- [9] N. Jamil, A.R. Yusoff and M.H. Mansor, "Experimental study of the static modal analysis on milling machine tool," *Adv. Mater. Res.*, vol. 903, 2014, pp. 123–128.
- [10] A. M. Avossa and G. Pianese, "Damping effects on the seismic response of base-isolated structures with LRB devices," *Ingegneria Sismica*, vol. 34, 2017, pp. 3–29.
- [11] W.-H. Lin and A. K. Chopra, "Earthquake response of elastic sdf systems with non-linear fluid viscous dampers," *Earthq. Eng. Struct. Dyn.*, vol. 31(9), 2002, pp. 1623–1642.
- [12] N. Nakamura, "A practical method to transform frequency dependent impedance to time domain," *Earthq. Eng. Struct. Dyn.*, vol. 35, 2006, pp. 217–231.
- [13] J. Galos, A.K. Akbar and M. P. Adrian, "Vibration and acoustic properties of composites with embedded lithium-ion polymer batteries," *Compos. Struct.*, vol. 220, 2019, pp. 677–686.
- [14] S. Pedrammehr, H. Farrokhi, A.K.S. Rajab, S. Pakzad, M. Mahboubkhah, M.M. Ettefagh and M.H. Sadeghi, "Modal analysis of the milling machine structure through FEM and experimental test," *Adv. Mater. Res.*, vol. 383–390, 2012, pp. 6717–6721.
- [15] Z. Lu, B. Huang, Q. Zhang and X. Lu, "Experimental and analytical study on vibration control effects of eddy-current tuned mass dampers under seismic excitations," *J. Sound Vib.*, vol. 421, 2018, pp. 153–165.
- [16] W. Wang, X. Wang, X. Hua, G. Song and Z. Chen, "Vibration control of vortex-induced vibrations of a bridge deck by a single-side pounding tuned mass damper," *Eng. Struct.*, vol. 173, 2018, pp. 61–75.
- [17] C.C. Chang, R.A. Kumar and M.M. Bernitsas, "VIV and galloping of single circular cylinder with surface roughness," *J. Ocean Eng.*, vol. 38(16), 2011, pp. 1713–1732.
- [18] K. V. Vidyanandan and S. Nilanjan, "Primary frequency regulation by de-loaded wind turbines using variable droop," *IEEE Transactions on Power System. Eng.*, vol. 29(4), 2014, pp. 1145–1154.
- [19] L. Bondioli, P. Raia, P. O'Higgins and D. Marchi, "morphomap: An R package for long bone landmarking, cortical thickness, and cross-sectional geometry mapping," *Am. J. Phys. Anthropol.*, vol. 174, 2021, pp. 129–39.
- [20] W. Zhao and J. Huang, "Boundary treatment of implicit-explicit Runge-Kutta method for hyperbolic systems with source terms," *J. Comput. Phys.*, vol. 423, 2020, pp. 109828.

## Contribution of individual authors to the creation of a scientific article (ghostwriting policy)

Valentin Eremin developed the concept and methodology of the study  
Alexander Bolshikh carried out finite element modeling and wrote the text

## Sources of funding for research presented in a scientific article or scientific article itself

Not applicable

## Creative Commons Attribution License 4.0 (Attribution 4.0 International , CC BY 4.0)

This article is published under the terms of the Creative Commons Attribution License 4.0

[https://creativecommons.org/licenses/by/4.0/deed.en\\_US](https://creativecommons.org/licenses/by/4.0/deed.en_US)